SYNOPSIS OF THE THESIS ENTITLED

Reconstruction of water-column temperature variability in the Eastern Arabian Sea from the Last Glacial Maximum to Holocene by Mg/Ca of planktic and benthic foraminifera

Proposed to be submitted in

the fulfillment of the requirements for the Degree of

DOCTOR OF PHILOSOPHY

in Marine Geology

submitted to

MANGALORE UNIVERSITY

by

Rajasree A
Research scholar

Under the guidance of

Dr. V. K. Banakar

Chief Scientist (Retired)
CSIR-National Institute of Oceanography,
Dona Paula, Goa - 403004, India

Department of Marine Geology
Mangalore University
Mangalagangotri-574199

November 2021

Introduction

Reconstruction of the past-ocean climatology is necessary to understand the link between Ocean and climate change. As the future climate is dominated by the human activities superimposed on natural climate, the subtraction of the latter from the composite (resultant) effect is a necessity. The prediction models for future climatic variations require information on natural background climate conditions. For understanding the past changes on various time-scales we require suitable and reliable proxies. Such proxies are present in the oceanic sediments deposited over the time. One of such several proxies is a group of micro-organisms known as foraminifera which secrete calcite tests mostly in equilibrium with ambient water (Hemleben et al., 1989). It means, they incorporate the temperature-salinity and isotopic signatures of the water in to their calcite test during their life time and on death settle to the seafloor instantly and become part of the sediment.

The foraminifera are largely grouped as planktonic (free-floaters, dwelling in euphotic waters) and benthic (sessile organisms, bottom dwelling). Another striking aspect of the planktonic foraminifer ecology is that they live over a range of depths in the upper part of the oceanic water column with individual species showing depth preferences (Farmer et al., 2007, see Figure 1), hence record the water properties of their respective habitat depths. On the other hand, the benthic foraminifera (epifaunal or infaunal) are sessile organisms which utilize the sedimentary organic matter as their food source and record the properties of bottom waters. These various potential properties of the foraminifera make them useful tools for understanding the past changes in climatic conditions via the oceanic waters.

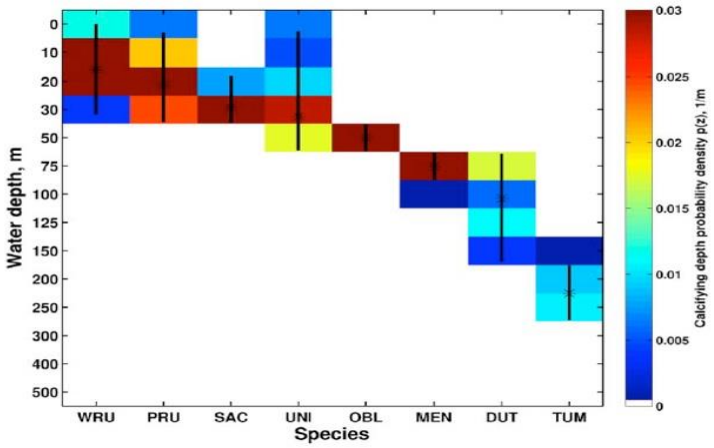

Figure 1: Various planktonic foraminiferal calcification depth. * = mean habitat depth in m. WRU, *G. ruber* (white); PRU, *G. ruber* (pink); SAC, *G. sacculifer* (without final chamber); UNI, *O. universa*; OBL,*P.obliquiloculata*; MEN, *G. menardii*; DUT, *N. dutertrei*; and TUM, *Gr. tumida*. (Figure source Farmer et al., 2007)

Geochemists have recognized a potential relationship between Mg/Ca in foraminiferal shells and ambient water temperatures. So, the application of Mg/Ca thermometry to multiple

species of planktonic foraminifera within a given sediment core can provide a powerful tool for reconstructing changes in water column properties (Regenberg et al., 2009; Cleroux et al., 2013). For example, *G. ruber* (white variety) and *G. sacculifer* species may be used for surface and mixed layer properties, while *N. dutertrei g*enerally represents upper thermocline conditions (Farmer et al., 2007; Spero et al., 2003). The Mg/Ca temperatures along with $\delta^{18}O_{foram}$ will provide a means to estimate $\delta^{18}O_{seawater}$ (Epstein et al., 1953), which is dependent upon the salinity (Delaygue et al., 2000).

I have carefully selected three planktonic species each from mixed layer (*G. sacculifer:* calcification depth ~30 m: Farmer et al., 2007), from upper thermocline (*N dutertrei:* calcification depth ~100 m: Farmer et al., 2007), from the base of the photic zone or lower themocline at ~200 m water depth (*Gr. tumida:* Ravelo and Fairbanks, 1992; Wara et al., 2005), and a deepwater benthic foraminifera *Uvigerina* species.

The SSTs (or mixed layer temperature) of the Arabian Sea on one hand decides the intensity of summer monsoon wind intensity and moisture load in the summer atmosphere, while on other hand it instantly responds to Indian monsoon system (summer and winter monsoons). The temperature changes at depths below the mixed layer are due to changes in intermediate and deep-water circulations independent of the local climatology.

The production of intermediate and deep-water masses in the high latitudes during the past have been reported by many researchers as a cause or effect of climate change (Piotrowski et al., 2009; Robinson and van de Flierdt, 2009; Pena and Goldstein, 2014) and these remote waters do reach the northern Indian Ocean at different depths. Therefore, thermal structure at a given location in the Arabian Sea may have a link with these remote waters.

Objectives

A significantly different surface climatology in the Eastern Arabian Sea (EAS) during LGM when compared to the Holocene have been suggested in several previous studies (Chodankar et al., 2005; Govil and Naidu, 2010; Mahesh et al., 2011; Banakar et al., 2010). Although there have been several Mg/Ca-Sea Surface Temperature (SST) reconstructions for the Arabian Sea (Anand et al., 2003; Banakar et al., 2010; 2017; Dahl and Oppo, 2006; Kessarkar et al., 2013; Saher et al., 2007; Saraswat et al., 2005), the reconstruction of the entire water column temperature utilizing a set of depth-specific foraminifera species are not available. Hence, the behaviour of water column temperature structure with respect to past climate variation is not clearly known. The past variation in the thermal structure of the water-column can provide useful information on the connection between monsoon forced surface

climatology with the global climate forced deep-water behaviour in the Arabian Sea, which is yet unclear (Schmiedl and Leuschner, 2005). The past deep-water circulation has been modulated by the global climate (Broecker and Denton, 1989; Waelbroeck et al., 2002). The past changes in the Indian summer monsoons (ISM) also have been shown to have connected to global climate variability both on glacial-interglacial time-scale (Banakar et al., 2010; Sijinkumar et al., 2016; Wang et al., 2001; Burns et al., 2003) and also on Dansgaard-Oeschger time-scale (Schulz et al., 1998; Kudrass et al., 2001; Kessarkar et al., 2013). In the modern times, the relative depth of mixed layer and thermocline vary with the reversing monsoon winds and their strength (Ramesh and Krishnan, 2005; Shetye, 1986). The thermocline dynamics has an important role in the surface productivity of the Arabian Sea. Thus, by utilizing the reconstructed temperatures at different depths recorded in depth specific planktic species, the temperature gradient between the mixed layer and thermocline can be calculated, which in turn can provide variation in the thermocline depth occurred in response to global climate change. Thus, the key objectives of the study are as follows.

- To reconstruct water column temperature from Mg/Ca ratios in selected foraminifera species characteristic of mixed layer, thermocline and bottom water.
- To understand the changes occurred in the circulation pattern from Last Glacial Maximum to Holocene and local climatological perspective vis-à-vis global climate variability.

Study area

The Arabian Sea is western basin in the tropical northern Indian Ocean, which is significantly influenced by the seasonally reversing monsoon winds. The seasonal monsoon winds cause significant changes in the SST, Surface Salinity and biogeochemistry in this basin. The intense coastal upwelling off Oman Margin and winter mixing off Makran Coast of this basin brings nutrient rich subsurface water to the surface making it one of the most productive regions in the world (Shankar et al., 2002; Madhupratap et al., 1996; Haake et al., 1993). Most of the Indian Summer Monsoon (ISM) associated rainfall on the Western Ghats quickly drains into the coastal Arabian Sea through numerous mountain rivers and streams. There is a sharp north-south gradient in the ISM rainfall along the west coast. For example, at Mangalore (~12.5ºN) the annual average rainfall is as high as 4000 mm, while in north, at Saurashtra and Kutch it is only 300 mm. This north-south gradient (~350 mm/deg latitude) results in variations in the river discharge to the EAS and hence, plays an important role in determining the surface salinity in the Eastern Arabian Sea (EAS).

The hydrography of Arabian Sea is characterized by water masses originated from Atlantic, Antarctic and Persian Gulf and Red Sea. The surface layer is characterised by the presence of Arabian Sea High Salinity Water mass (ASHSW), which is formed during winter as a result of enhanced evaporation in the northernmost part of the basin. This water mass subsequently spreads southward with increasing depth of penetration and found in the EAS just below the slightly lower salinity mixed layer. The mixed layer in the EAS is composed of a mixture of extremely low-salinity water of BoB flowing in to the EAS as poleward coastal currents in winter, water from mountain river discharge and clockwise spreading of upwelled water off Oman during summer.

The thermocline of the Arabian Sea is ventilated by a mixture of remotely sourced waters such as Persian Gulf Water (PGW), Red Sea Water (RSW), Subantarctic Mode Water (SMW), Antarctic Intermediate Waters (AAIW) (Fine et al., 2008; You, 1998). The RSW and PGW are significantly warmer and saline waters compared to SMW and AAIW. The mixture of all these waters collectively termed as Indian Central Water (ICW). The deep water below the thermocline is composed of a mixture of aged NADW and CDW extending from 1200 m to 3800 m and is commonly referred as North Indian Deep Water (NIDW) (van Aken et al., 2004; You, 1998; Ziegler et al., 2010).

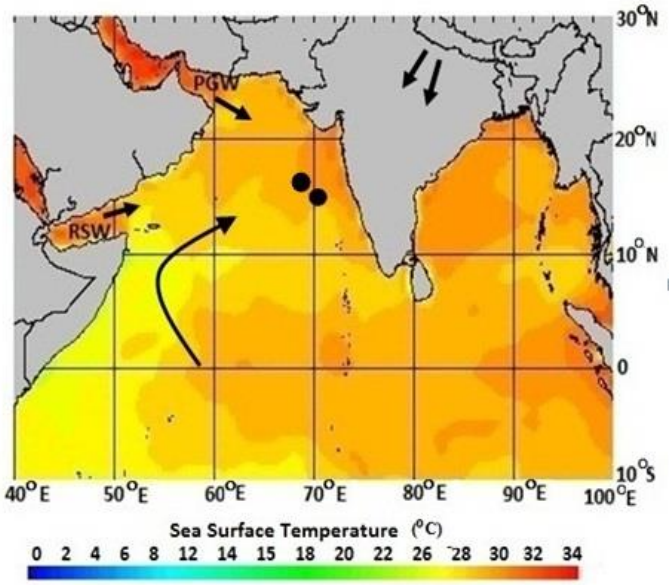

Figure 1. Location of the studied sediment cores BP3-GCR01and BP3-GCR02 (filled circle) shown on the annual sea surface temperature map. (Source:www.globalweathersystems.com). Red Sea Water (RSW) and Persian Gulf Water (PGW) outflow into the Arabian Sea thermocline is shown with arrows. General direction of Indian summer monsoons is shown with curved upward arrow and winter monsoons with short downward arrows

Material and Methods

Two sediment cores from the Eastern Arabian Sea have been utilized for the present study. The first core BP3-GCR01 (15°31' N; 70°05' E) is from a water depth of 1500 m and is taken from the top of Wadia Sea mount. The second core BP3-GCR02 (17°10.5'N ;69°00.5' E) is from 2400 m water depth; which is taken from the top of Raman Seamount. Both the cores are AMS-Radiocarbon dated. These cores have already been sub sampled at 1 cm intervals. The planktonic foraminifera *G. sacculifer, N. dutertrei, and Gr. tumida,* and benthic foraminifera *Uvigerina* spp were selected for the present study. For Mg/Ca analyses, the hand-picked tests of foraminifera were cleaned both physically and chemically. The cleaning was done by following the cleaning protocol developed by Barker et al. (2003). The cleaned tests were dissolved in 0.075 M HNO_3 and the resulting solutions analyzed for Mg, Ca, Al, Mn and Fe following standard calibration. The Mg/Ca (mmol/mol) was estimated following Intensity Ratio Calibration against known Mg/Ca (mmol/mol) calibration standards.

The Mg/Ca measurement was carried out at CSIR-National Institute of Oceanography, Goa on Perkin-Elmer Optima 7300 DV simultaneous Inductively coupled plasma optical emission spectroscopy (ICP-OES) following intensity-ratio calibration technique developed by DeVilliers et al. (2002), while the contaminant monitoring elements (Al, Fe, and Mn) were measured following standard multi element calibration method. The concentration of Ca was checked after every analysis and high Ca concentration solutions were diluted to ~70 ppm by adding 0.075 M suprapure HNO_3 and reanalyzed whereas extremely low Ca (< 40 ppm) containing sample solutions were either not used or prepared again. It is because of the reason that in IR calibration method, most consistent ratios with highest precision were obtained when the Ca content in the solutions was 50 to 80 ppm (De Villiers *et al.*, 2002). Hence, the solutions with extremely low Ca (< 40 ppm) were either not used or were again prepared, while solutions with high Ca were diluted to —70 ppm level and reanalyzed. The IRs obtained for five standards containing variable Mg/Ca (mmol/mol) were used to establish IR calibration. Then the Mg/Ca IRs of sample solutions were converted in to Mg/Ca (mmol/mol) ratios using this calibration. In order to validate the long-term stability in the instrumental conditions a quality control (QC) solution of known Mg/Ca was repeatedly measured after every six-sample solution. The deviations of the QC from its known values were calculated and utilized to correct the Mg/Ca obtained for sample solutions following step-correction. This approach ensures that the reported Mg/Ca are free from minor fluctuations due to instrumental-drift. The Mg/Ca for every solution is the average of five replicate measurements. The presence of high levels of Fe

and Al can increase the values of Mg/Ca ratios (Barker *et al.*, 2003). Hence, the solutions containing > 0.03 mmol/mmol of Al or Fe or Mn / Mg ratios were rejected or samples were prepared again following all the cleaning procedures. The Mg/Ca ratios were converted into calcification temperatures using species-specific Mg/Ca-Temperature calibrations (*G. sacculifer*: Dekens et al., 2002; *Gr. tumida*: Rickaby and Halloran, 2005; *Uvigerina* spp: Lear et al., 2002). The $\delta^{18}O$ and $\delta^{13}C$ analyses was carried out at IsoLab, University of Washington, USA, where Finnigan DeltaPlus coupled with Kiel III carbonate system calibrated with NBS19 (white marble) and NBS18 (carbonatite) was used. The $\delta^{18}O_{Seawater}$ was calculated from the paleotemperature equation (Bemis et al., 1998) from sea level corrected $\delta^{18}O_{G.sacculifer}$ and measured Mg/Ca-Temperatures. The sea surface salinity was estimated from $\delta^{18}O_{Seawater}$ – salinity empirical equation derived for the Arabian Sea [$S = (\delta^{18}Osw + 20)/0.57$: Dahl and Oppo, 2006]. The abundance of *Uvigerina* spp. is estimated by counting the number of *Uvigerina* tests in one gram of the coarse fraction under microscope. The size fraction between 150-355 μm was used.

Results and conclusions

The radiocarbon ages for BP3-GCR01 and BP3-GCR02 covers the last 35 and 32 ky respectively. The $\delta^{18}O_{G.sacculifer}$ of both the core exhibit a clear glacial- interglacial trend with heaviest $\delta^{18}O$ occurred during LGM and the lightest $\delta^{18}O$ during Holocene. In the sediment core BP3-GCR01, depleted $\delta^{18}O_{G.sacculifer}$ (− 0.9 to − 1.3 ‰) are observed in sections between 11 ka and 5 ka) that marks the warmest Holocene climate and the enriched $\delta^{18}O_{G.sacculifer}$ (+0.02 to + 0.35‰) are observed between ~ 28 to 20 ka indicating the coldest LGM climate (Figure 2). The depleted $\delta^{18}O_{G.sacculifer}$ (−1.24 to − 1.3 ‰) in the core BP3- GCR02 is observed between 10 ka and 5 ka) and the enriched $\delta^{18}O_{G.sacculifer}$(+0.6 to – 0.0‰) is observed between 19 ka and 28 ka. The deglacial period (19 ka to 11 ka) in both the sediment core is marked by the sharp decrease in $\delta^{18}O_{G.sacculifer.}$ The results are in good agreement with the previous $\delta^{18}O$ records from the EAS (Banakar et al. 2005; Chodankar et al. 2005). The LGM - Holocene $\delta^{18}O_{G.sacculifer}$ contrast (difference between highest and lowest $\delta^{18}O$) in BP3-GCR01 and BP3-GCR02 is around ~1.5 ‰. The effect of global ice volume or sea level on oceanic $\delta^{18}O$ equivalent to 1 ‰ (Duplessy, 1982; Shackleton, 2000) when subtracted from the obtained LGM - Holocene $\delta^{18}O_{G.sacculifer}$ contrast yields 0.5 ‰ in excess that cannot be accounted by global climate change. This excess of 0.5 ‰ therefore should reflect the local salinity effect.

The $\delta^{18}O_{N.dutertrei}$ representing upper thermocline water change from ~1.2 ‰ during the LGM to −0.6 ‰ during the Holocene. Similarly, the $\delta^{18}O_{Gr.\ tumida}$ representing the lower thermocline water changes from 0.5 ‰ to −0.9 ‰ (Figure 4). That is, a decrease of ~ 1.8 ‰ in upper thermocline and ~1.4 ‰ in the lower thermocline, as a result of climate transition from cold LGM to warm Holocene. After subtracting global effect of 1 ‰ from these changes, the upper thermocline water appears to have witnessed ~0.8 ‰ excess and lower thermocline waters have witnessed ~0.4 ‰ excess $\delta^{18}O$ change. At the outset the larger change in the upper thermocline may be because of its effective communication with the overlying mixed layer that is instantly responds to monsoon system. Therefore, large effect of changes in E-P could be transferred from mixed layer $\delta^{18}O$ to upper thermocline $\delta^{18}O$. On the other hand, small excess of ~0.4 ‰ change in the lower thermocline suggest its affinity towards intermediate water, which are insulated from the monsoon effect, and carry $\delta^{18}O$ change equivalent to global ice volume effect of 1 ‰. Thus, the $\delta^{18}O$ in upper thermocline water tends towards mixed layer character having local climate effect superimposed on the global climate change, while the lower thermocline waters tend towards intermediate water isotopic characters, which reflect only global climate change.

A comparison of the $\delta^{18}O_{G.sacculifer}$ $\delta^{18}O_{N.dutertrei}$ and $\delta^{18}O_{Gr.\ tumida}$ time-series of the present sediment cores with the SPECMAP (Imbrie et al., 1984), LR04 Benthic stack (Lisiecki and Raymo, 2005), GISP2 ice-core (Greenland) (Grootes and Stuvier, 1997, Grootes et al., 1993) and EDML ice-core (Antarctica) (EPICA community members, 2010) records, indicate that the EAS $\delta^{18}O_{FORAMINIFERA}$ are remarkably coherent with global $\delta^{18}O$ records.

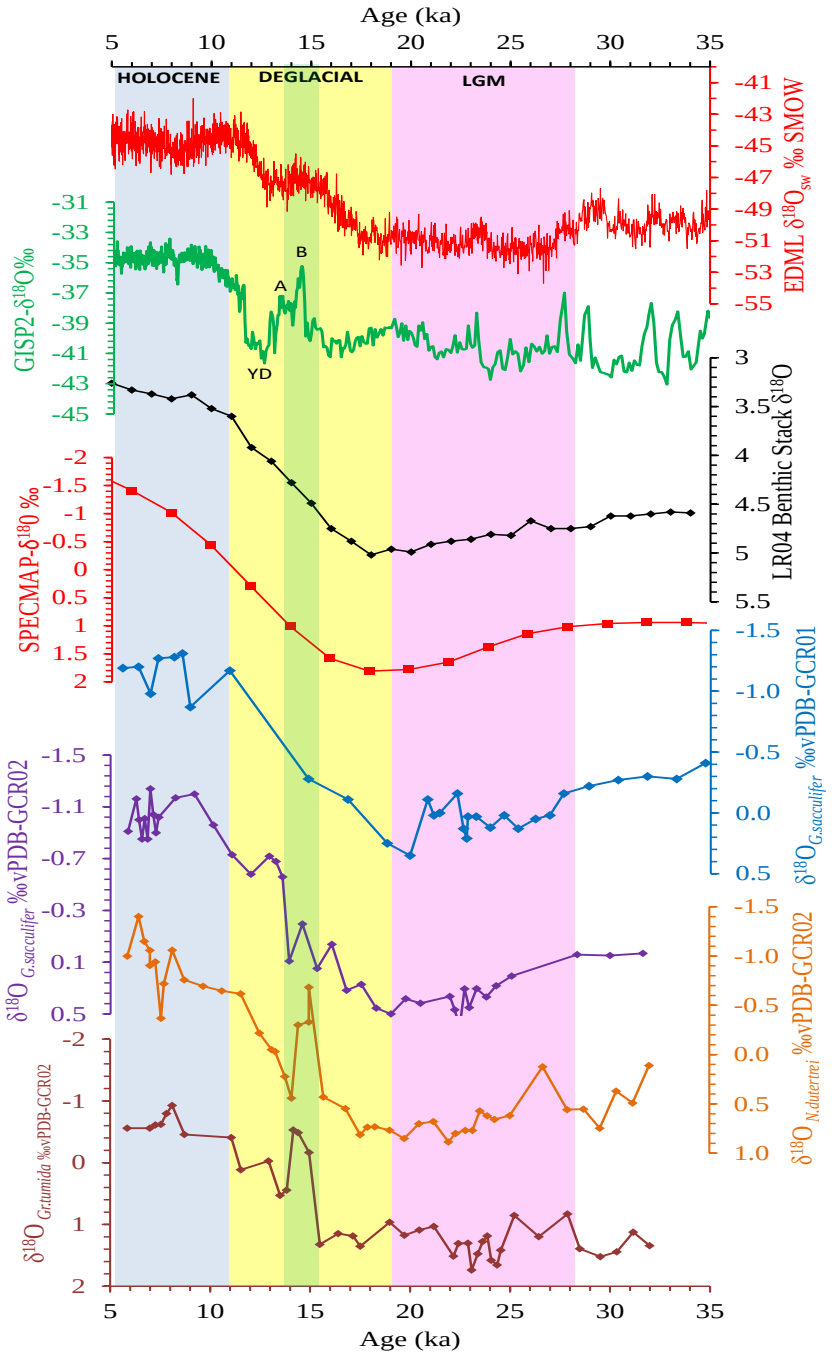

Figure 2. The time-series of $\delta^{18}O$ records of the planktic foraminifera (upper water column) compared with global climate records of northern and southern hemisphere. Red curve - SPECMAP planktic Oxygen Isotope Stack of marine sediment (Imbrie et al., 1984) Black curve - LR04 benthic Oxygen Isotope Stack of marine sediments (Lisiecki and Raymo 2005), GISP2 ice-core (Greenland) (Grootes and Stuvier, 1997) and EDML ice-core (Antarctica) (EPICA community members, 2010). Pink shaded bar is LGM, Yellow colour bar is Deglaciation, Blue shaded bar is Holocene, and Green shaded bar is Bolling – Allerod (BA) warm event.

Water column thermal structure

The reconstructed SST variation shows that the Eastern Arabian was ~2 °C colder during Last Glacial Maximum (LGM) when compared with the Holocene (Figure 3). The observed SST variation is consistent with previously published LGM-Holocene SST gradient of < 3 °C (Rostek et al., 1993; Sonzogni et al., 1998; Cayre and Bard, 1999; Saraswat et al., 2005; Banakar et al., 2010). The SST of EAS is mainly dependent on seasonally reversing monsoon winds. Most of the researchers have reported strengthened winter monsoon (in turn sea surface cooling) during the LGM. The prolonged and strengthened winter monsoon resulted in the cooling of SST in the Arabian Sea (Fontugne and Duplessy, 1986). These observations suggest that the EAS SST variability is controlled by its own internal forcing rather than the global temperature influence.

The thermocline temperatures also show lowering by 3 – 4 °C (Figure 3). Even though there are minor fluctuations in the time series, a warming trend in two steps can be clearly seen (from ~30 ka to 20 ka, and ~15 ka to ~8 ka). The thermocline temperature reconstructed by Rippert et al. (2015) also suggested a cooling of 3.5 °C in the tropical Western Indian Ocean. Any changes in the thermocline property are an indication of the changes occurred in the water mass at that depth. The thermocline of the Arabian Sea is ventilated by the water masses of distant origins. Thus, the thermocline cooling observed here is suggestive of the changes occurred in the intermediate circulation during LGM. Several studies have demonstrated a different hydrography of intermediate depths of Indian Ocean during LGM (Kiefer et al., 2006; Jung et al., 2009; Wang et al., 2013; Romahn et al., 2014). The lowering of the sea level during LGM has been suggested to have a major impact on the circulation of the thermocline watermass. The PGW and RSW are separated from the open oceans by shallow and narrow sills, viz., Strait of Hormuz (50 m sill depth) and the Strait of Bab-el-Mandeb (137 m sill depth) respectively (Rohling and Zachariasse, 1996). A lowering of the global sea level by 120 m during the LGM has not only caused a significant reduction in the outflow of RSW into the Arabian Sea, but also caused total cut-off of the PGW supply (Fairbanks, 1989; Siddall et al., 2003). This reduction must have to be compensated for maintaining the mass-balance at the thermocline depth, which appears to have been compensated by the enhanced supply of glacial-AAIW (GAAIW) (Jung et al., 2009) or increased supply of SMW. Although, presently the presence of AAIW is observed only up to 10 ºS in the Indian Ocean (Lynch-Stieglitz et al., 1994), an enhanced production during glaciation have spread the AAIW in the entire Indian

Ocean (Bryan et al., 2010). Similarly, a more northward propagation of AAIW during deglaciation was also reported in the Atlantic Ocean (see Pahnke et al., 2008) and in Pacific Ocean (see Basak et al., 2010).

The BWT vary between ~10 °C and ~6 °C from 10 ka to 35 ka (Figure 3). The bottom water record of the core GCR01 shows a general lowering of temperature during the LGM even though several fluctuations are observed throughout (Figure 3). As this sediment core captures the temperature changes at ~1500 m, the deepwater reaching this location were inherently 3 - 4 ^{o}C colder during the LGM. In the EAS, 1 - 2 km depth is flooded by a mixture of aged NADW and CDW (Kallel et al., 1988; You, 2000; Van Aken et al., 2004). A reduction in the production of NADW during the LGM has been reported by several researchers (Duplessy et al., 1988; Bickert and Mackensen, 2003; Curry and Oppo, 2005). Then what should be the cause of this 4 ^{o}C cooling at 1.5 km depth in the EAS. The likely scenario would be, when the NADW production was reduced during LGM, the production of deepwater waters at the Antarctic margins might have enhanced, which appear to have replaced the shortage of NADW in the EAS. This might have led to enhanced proportion of southern sourced water at depth in the EAS maintaining the LGM cooling signal. There are a few published records which reported reduction in deep water ventilation in the Indian Ocean during LGM (Duplessy et al.,1988; Kallel et al., 1988; Raza and Ahmad, 2013). A similar glacial deepwater cooling of ~ 2 °C has already been reported for the northeast Indian Ocean (Raza and Ahamad., 2013). Kallel et al. (1988) observed that the glacial deepwater of Indian Ocean was 1.5 °C colder and was poorly oxygenated and depleted in δ^{13}C when compare to the Present. An anoxic condition during the last glacial period was identified by Sarkar et al (1993) in the Eastern Arabian Sea and the probable condition for such an oxygen depleted condition is explained as the change in the deep-water circulation. Thus, the observed drop in the bottom water temperature during LGM suggest that a relatively colder deepwater formed at Antarctic margin might have dominated the CDW to compensate for the reduced NADW resulting in increased cooling of the deep water in EAS.

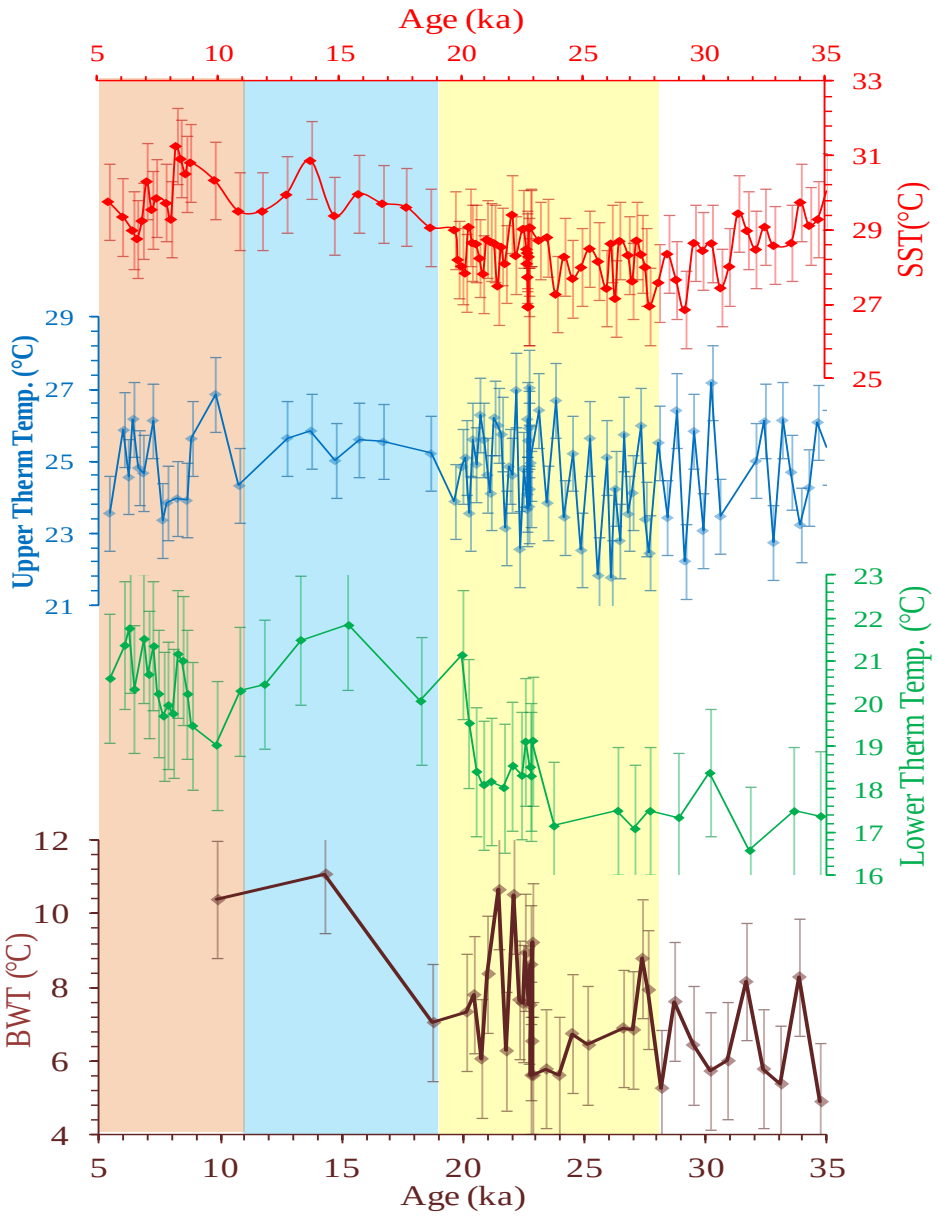

Figure 3. Composite of past temperature variation at different depths in water column of the Eastern Arabian Sea estimated from Mg/Ca of foraminifera from the core BP3-GCR01; SST = sea surface temperature estimated from *G. sacculifer*, UTT & LTT = upper and lower thermocline temperature estimated from *N. dutertrei* and *Gr. tumida respectively*, BWT = bottom water temperature at 1500-m water depth estimated from *Uvigerina* spp in the sediment core location. The 1 σ error in each time series is shown with capped vertical lines. Color-shaded vertical bars are different climate stages viz., yellow = LGM; blue = deglaciation; pink = Holocene.

Thermal gradient between sea surface and lower thermocline and its implications

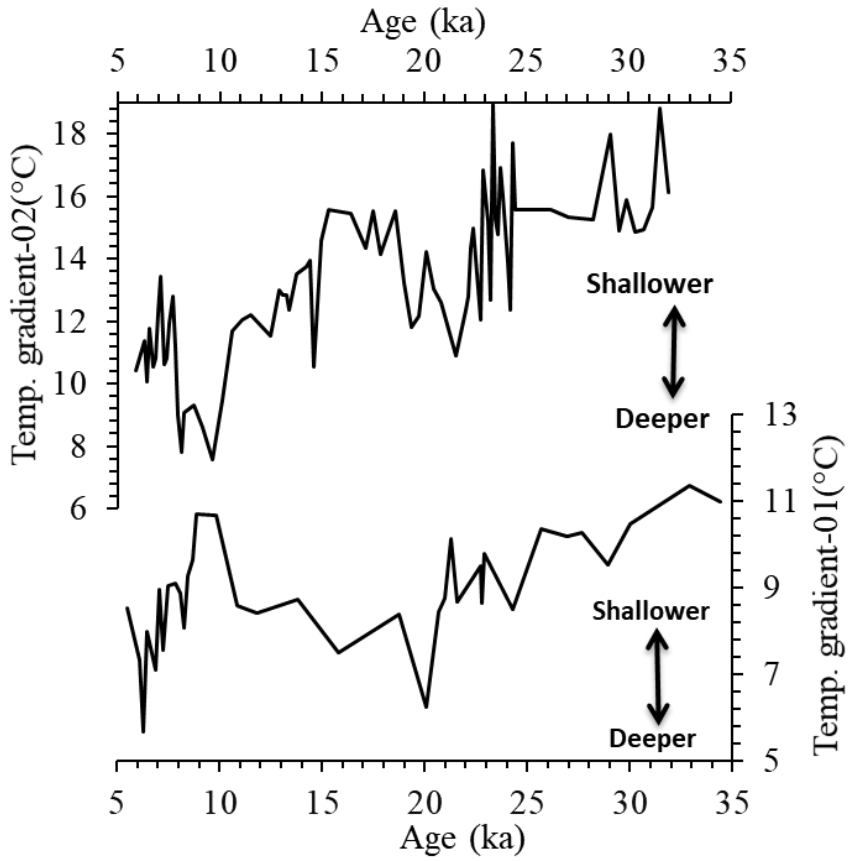

Figure 4. Temperature gradient between surface and the lower thermocline indicating the dynamics of the thermocline from the sediment core BP3-GCR01 (Lower panel) and BP3-GCR02 (Upper panel).

The temperature gradient (ΔT) between the surface and the Lower thermocline shows glacial –interglacial trend, even though there are some fluctuations. This indicate that the thermocline depth was affected by the glacial-interglacial climatic conditions. The temperature gradient is observed to be decreasing from 35 ka to 5 ka. The ΔT is observed to be >9 °C throughout the LGM in both the sediment core (Figure 4). A large difference between the mixed layer and thermocline (ΔT) indicates a shallower thermocline whereas a low ΔT indicates a deeper thermocline (Rippert et al., 2015). Thus, it is clear that the thermocline in the EAS was shallower during LGM and deeper during the Holocene. This observation is already presented (see Rajasree et al., 2019) and is also supported by the previous study from the Western Tropical Indian Ocean (Rippert et al., 2015).

The increased ΔT during the LGM suggests an intensified winter monsoon which caused the shoaling of mixed layer and thermocline. This finding is in excellent agreement with the modeling study by Liu et al., 2007, which show that the weakened Asian monsoon during glacial times resulted in a significant shoaling of the mean tropical thermocline in the

central and western Indian Ocean. The intensified winter monsoon in the EAS during LGM has been reported in many studies (Anderson and Prell, 1993; Rostek et al., 1997; Clemens and Prell, 2003; Banakar et al., 2005). A decreased summer monsoon during the LGM has been a cause for an increased stratification of the upper water column (Huguet et al., 2006). The shallower thermocline during LGM might have contributed to the high productivity by supplying the nutrients to the surface via deep convective mixing.

Uvigerina abundance and the productivity changes

The infaunal benthic foraminifera, *Uvigerina* spp abundance was studied in order to understand the changes occurred in the surface productivity from LGM to Holocene in the Eastern Arabian Sea. The LGM interval at both the core location is marked by high abundance of *Uvigerina* spp. (figure 5). Distinct abundance minima were observed in both the sediment cores during the Holocene and deglaciation period. The *Uvigerina* spp. as mentioned before is an infaunal benthic foraminifera species and it occupy the near sediment-water interface (0- 1 cm) (Corliss and Emerson, 1990). There are several studies which shows the high abundance of *Uvigerina* are associated with high surface productivity and organic carbon rich bottom water sediments (Altenbach and Sarnthein, 1989; Boersma, 1985; Corliss et al., 1986; Lutze, 1986; Woodruff, 1985). Studies have also reported the high abundance of *Uvigerina* is linked with oxygen poor environments. The flux of organic carbon to the sea floor and the dissolved oxygen concentration in the deep water are considered as the two important factors which affects the abundance pattern of *Uvigerina* spp and these factors are inter- related. Studies have been conducted in the EAS to understand how the abundance of benthic foraminifera and changes in the dissolved oxygen concentration are related (Den Dulk et al. 2000; Schumacher et al. 2007). The high flux of organic carbon is a result of high surface productivity and this high flux of organic carbon leads to high consumption of dissolved oxygen by the microbes for the decomposition (Jorissen et al., 1995; Bernhard and Sen Gupta, 1999). This in turn causes low dissolved oxygen concentration in the Bottom waters.

The comparison of abundance data of *Uvigerina* spp. with the C_{org} and total n-alkanes data (Punyu PhD thesis, 2015) shows an excellent agreement and exhibit near similar enrichment through most of the LGM (Figure 13). Thus, it can be said that the export production in the EAS was significantly higher during the LGM, which is consistent with previous observations from this region (Banakar et al., 2005).

The abundance of *Uvigerina* spp. C_{org} and total n-alkanes data clearly suggest high productivity in the EAS during LGM (Figure 5). The high productivity during LGM may have been caused by increased organic carbon rain occurred in response to the high surface productivity in the EAS. This high productivity must be due to enhanced nutrient input in the surface water by intensified NE monsoon winds (Pourmand et al., 2007; Rajasree et al., 2019; Rostek et al., 1997; Madhupratap et al. 1996). Previous palaeoceanographic studies in the EAS also have suggested that productivity in the region have increased during the LGM (Cayre and Bard 1999; Singh et al., 2011; Rostek et al., 1997; Banakar et al., 2005) and the increased productivity was explained in terms of intensified winter monsoon causing enhanced deep convective mixing which finally results in more nutrient injection to the surface water (Pourmand et al. 2007; Rostek et al. 1997). The high surface water productivity leads to high export production and high oxygen demand driven by remineralization of organic matter resulting in an anoxic condition leading to enhanced preservation of organic matter (Deplazes et al.,2014).

The comparison of *Uvigerina* abundance from both the sediment core with the total organic carbon (%TOC) from the northern Arabian Sea sediment core (Reichart et al., 1998) and the *Uvigerina* abundance % from the western Arabian Sea (Schmiedl and Leuschner, 2005) shows good agreement with similar patterns of variability in all the records (Figure 5). The peak abundance of *Uvigerina* in the present study as well as in western Arabian Sea record during last glacial period is corresponded with high TOC % in the northern Arabian Sea. The total organic carbon concentration in the marine sediment is a widely used proxy for surface productivity with high value of TOC indicating high surface productivity (Reichart et al., 1997; Schulz et al., 1998; von Rad et al., 1999). High surface productivity results in increased organic matter flux to the seafloor.

This striking similarities in the patterns of abundance of *Uvigerina* and TOC % from the EAS, western Arabian Sea and the northern Arabian Sea clearly suggest a basin -wide high productivity prevailed during last glacial period.

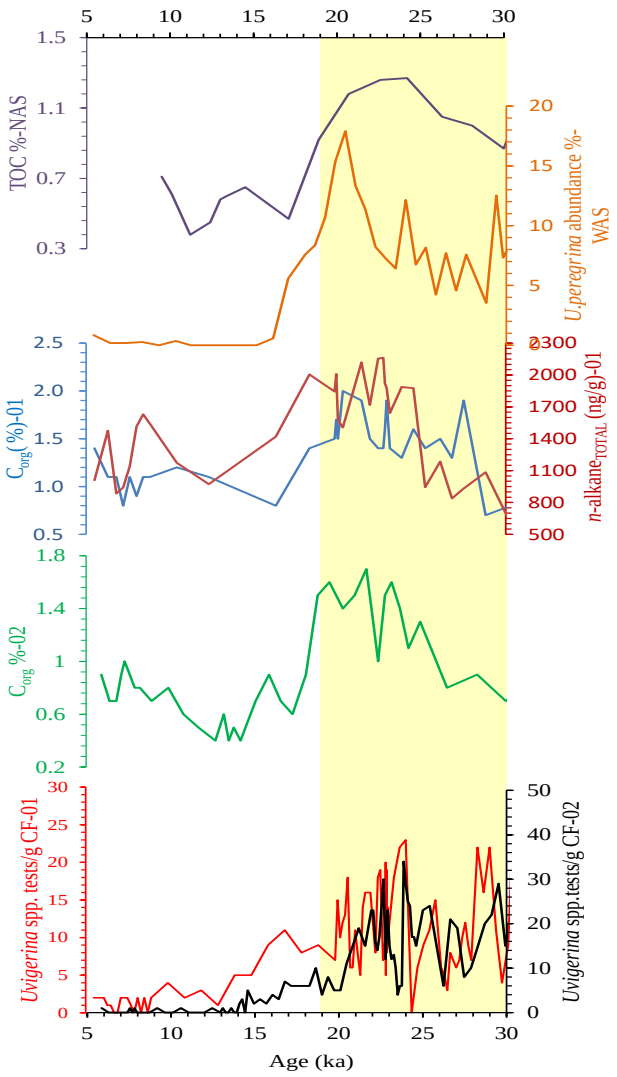

Figure 5. Comparison of *Uvgerina* abundance in BP3-GCR01 and BP3-GCR02 with other paleoproductivity records from the same sediment core Blue colour curve is the C_{org} % in BP3-GCR01, Purple colour curve is the n-alkane total record from the sediment core GCR01, Green colour curve is the Corg time series from the sediment core BP3-GCR02 (Punyu, 2015 PhD Thesis) and Violet colour curve is the total organic carbon (%TOC) from the northern Arabian Sea sediment core (Reichart et al., 1998), Orange colour curve is the *Uvigerina* abundance % from the western Arabian Sea (Schmiedl and Leuschner, 2005). Yellow shaded bar shows the Last glacial period.

The above presented aspects are the main components of the present thesis, that provides insight in to the climate dependent dynamics of the water column in the EAS. I have discussed in detail the cause and effect of changing thermal structure with depth in the EAS. The thesis is divided in to six sections starting from introduction and working hypothesis of my study, followed by results and discussion of reconstructed time-series, and closing with salient observations as conclusions. All the literature cited in the thesis is listed at the end under section 'References'.

Reference list

Altenbach, A.V., Sarnthein, M., 1989. Productivity record in benthic foraminifera. In: Berger, W.H., Smetacek, V.S., Wefer, G. (Eds.), Productivity of the Ocean: Present and Past. Wiley, New York, pp. 255–269.

Anderson, D.M., Prell, W.L., 1993. A 300 kyr record of upwelling off Oman during the late Quaternary: evidence of the Asian southwest monsoon. Paleoceanography 8, 193–208.

Banakar, V. K., Baidya, S., Piotrowski, A. M., Shankar D., 2017. Indian summer monsoon forcing on the deglacial polar cold reversals. J. Earth Syst. Sci. 26: doi: 10.1007/s12040-017-0864-5.

Banakar, V. K., Mahesh, B. S., Burr, G., Chodankar, A. R., 2010. Climatology of the Eastern Arabian Sea during the last glacial cycle reconstructed from paired measurement of foraminiferal δ18O and Mg/Ca. Quat. Res. 73, 535–540.

Banakar, V. K., Oba, T., Chodankar, A. R., Kuramoto, T., Yamamoto, M., Minagawa, M., 2005. Monsoon related changes in sea surface productivity and water column denitrification in the Eastern Arabian Sea during the last glacial cycle. Mar. Geol. 219, 99–108.

Barker, S., Greaves, M., Elderfield, H., 2003. A study of cleaning procedures used for foraminiferal Mg/Ca paleothermometry. Geochem. Geophys. Geosyst., 4, 8407.

Basak, C., Martin, E.E., Horikawa, K., Marchitto, T.M., 2010. Southern Ocean source of 14C-depleted carbon in the North Pacific Ocean during the last deglaciation. Nat. Geosci. 3, 770–773.

Bemis, B. E., Spero, H. J., Bijma, J., Lea, D.W., 1998. Reevaluation of the oxygen isotopic composition of planktonic foraminifera: experimental results and revised paleotemperature equations. Paleoceanography 13 (2), 150e160.

Bernhard, J. M., and Sen Gupta, B. K., 1999. Foraminifera of oxygen depleted environments; In: Modern Foraminifera (ed.) Sen Gupta B K, Kluwer Academic Publishers, Dordrecht.

Bickert, T., Mackensen, A., 2003. Last Glacial to Holocene changes in South Atlantic deep-water circulation, in the South Atlantic in the Late Quaternary. In: Wefer, G., Mulitza, S., Rathmeyer, V. (Eds.), Reconstrction of Material Budget and Current Systems. Springer, New York, pp. 671e693.

Boersma, A., 1985. Biostratigraphy and biogeography of Tertiary bathyal benthic foraminifera Tasman Sea, Coral Sea, and on the Chatham Rise (Deep Sea Drilling Project Leg 90). Init. Rep. DSDP, 90: 961-1035.

Broecker, W. S., Denton, G. H., 1989. The role of ocean-atmosphere reorganizations in glacial cycles. Geochimica et Cosmochimica Acta 53, 2465–2501.

Bryan, Sean P., Marchitto, Thomas M., Lehman, Scott J., 2010. The release of 14C- depleted carbon from the deep ocean during the last deglaciation: evidence from the Arabian Sea. Earth Planet. Sci. Lett. 298 (1–2), 244.

Burns, S. J., Fleitmann, D., Matter, A., Kramers, J., A. S. A. A., 2003. Indian Ocean climate and an absolute chronology over Dansgaard/ Oeshger Events 9 to 13. Science 301, 1365–1367, doi:10.1126/science.1086227.

Cayre, O., Bard, E., 1999. Planktonic foraminiferal and alkenone records of the last deglaciation from the eastern Arabian Sea. Quat. Res., 52, 337–342.

Chodankar, A. R., Banakar, V. K., Oba, T., 2005. Past 100 ky surface salinity gradient response in the Eastern Arabian Sea to the summer monsoon variation recorded by δ18O of G. sacculifer. Global Planetary Change 47, 135–142

Clemens, S. C. and Prell, W. L., 2003. A 350,000 year summer-monsoon multi-proxy stack from the Owen Ridge, Northern Arabian Sea. Marine Geology, 201(1): 35-51.

Cléroux, C., deMenocal, P., Arbuszewski, J., Linsley, B., 2013. Reconstructing the upper water column thermal structure in the Atlantic Ocean. Paleoceanogr. 28, 503–516, doi:10.1002/palo.20050.

Corliss B. H., and Emerson S.,1990. Distribution of rose-bengal stained deep-sea benthic foraminifera from the Nova Scotian continental margin and Gulf of Maine. Deep Sea Res. 37, 381–400.

Corliss, B. H., Martinson, D. G., Keefer, T., 1986. Late Quaternary deep-ocean circulation. Geological Society of America Bulletin 97, 1106–1121.

Curry, W. B., Oppo, D. W., 2005. Glacial water mass geometry and the distribution of $\delta^{13}C$ of CO_2 in the western Atlantic Ocean. Paleoceanogr., 20, 1–12. doi: 10.1029/2004PA001021.

Dahl, K. A., Oppo, D. W., 2006. Sea surface pattern reconstructions in the Arabian Sea. Paleoceanogr., 21, PA1014. doi:10.1029/2005PA001162.

De Villiers, S., Greaves, M., Elderfield, H., 2002. An intensity ration calibration method for the accurate determination of Mg/Ca and Sr/Ca of marine carbonates by ICP-AES. Geochemistry, Geophysics, Geosystems 3 (2001GC000169).

Dekens, P. S., Lea, D.W., Pak, D. K., Spero, H. J., 2002. Core top calibration of Mg/Ca in tropical foraminifera: refining paleo temperature estimation. Geochem. Geophys. Geosyst. 3 (4):1022. http://dx.doi.org/10.1029/2001GC000200.

Delaygue, G., Jouzel, J., Dutay, J. C., 2000. Oxygen 18–salinity relationship simulated by an oceanic general circulation model. Earth Planet. Sci. Lett. 178 (1–2), 113–123.

Den Dulk, M., G. J. Reichart, S. van Heyst, W. J. Zachariasse, and G. J. Van der Zwaan., 2000. Benthic foraminifera as proxies of organic matter flux and bottom water oxygenation? A case history from the northern Arabian Sea, Palaeogeogr. Palaeoclimatol. Palaeoecol., 161, 337–359.

Deplazes, G., Lückge, A., Stuut, J. B.W., Pätzold, J., Kuhlmann, H., Husson, D., Fant, M., Haug, G. H., 2014. Weakening and strengthening of the Indian monsoon during Heinrich events and Dansgaard-Oeschgeroscillations. Paleoceanography 29, 99–114.

Duplessy, J. C., Shackleton, N. J., Fairbanks, R. G., Labeyrie, L. D., Oppo, D., Kallel, N., 1988. Deepwater source variations during the last climatic cycle and their impact on the global deepwater circulation. Paleoceanogr., 3, 343–360.

Duplessy, J. C., 1982. Glacial–interglacial contrasts in the northern Indian Ocean. Nature 295, 494–498.

European Project for Ice Coring in Antarctica Community Members (EPICA)., 2010. Stable oxygen isotopes of ice core EDML. PANGAEA, doi:10.1594/PANGAEA.754444.

Epstein, S., Buchsbaum, R., Lowenstam, H. A., Urey, H. C., 1953. Revised carbonate-water isotopic temperature scale. Bulletin of the Geological Society of America 64, 1315–1325.

Fairbanks, R. G.,1989. A 17,000-year glacio- eustatic sea level record: Influence of glacial melting rates on the Younger Dryas event and deep-ocean circulation, Nature, 342, 637–642.

Farmer, E. C., Kaplan, A., de Menocal, P. B., Lynch-Stieglitz, J., 2007. Corroborating ecological depth preferences of planktonic foraminifera in the tropical Atlantic with the stable oxygen isotope ratios of core-top specimen. Paleoceanography 22, PA3205.

Fine, R. A, Smethie, W. M. Jr, Bullister J. L, Rhein M, Min, D. H, Warner, M. J, Poisson A, Weiss R. F., 2008. Decadal ventilation and mixing of Indian Ocean waters. Deep-Sea Res I Oceanogr Res Pap 55:20–37.

Fontugne, M. R., Duplessy, J. C., 1986. Variations of the monsoon regime during the upper Quaternary: evidence from carbon isotopic record of organic matter in north Indian Ocean sediment cores. Palaeogeogr. Palaeoclimatol. Palaeoecol., 56, 69–88.

Govil, P., Naidu, P. D., 2010. Evaporation-precipitation changes in the eastern Arabian Sea for the last 68 ka: implications on monsoon variability. Palaoecenography 25, PA1210. http://dx.doi.org/10.1029/2008PA001687, 2010.

Grootes, P., Stuvier, M., 1997. Oxygen 18/16 variability in Greenland snow and ice with 10−3 to 10−5 year resolution. J. Geophys. Res. 102, 26455–26470.

Grootes, P. M., Stuiver M, White, J. W. C, Johnsen S, Jouzel, J., 1993. Comparison of oxygen-isotope records from the Gisp2 and Grip Greenland ice cores. Nature 366:552–54.

Haake, B., Ittekkot, V., Rixen, T., Ramaswamy, V., Nair, R. R., Curry, W. B., 1993. Seasonality and interannual variability of particle-fluxes to the deep Arabian Sea. Deep-Sea Res. I 40, 1323–1344. http://dx.doi.org/10.1016/0967–0637(93)90,114.

Hemleben, C., and J. Bijma., 1994. Foraminiferal population dynamics and stable carbon isotopes, in Carbon Cycling in the Glacial Ocean: Constraints on the Ocean's Role in Global Change, edited by R. Zahn et al., pp. 145– 166, Springer, New York.

Huguet, C., Kim, J. H., Sinninghe Damsté, J. S., Schouten, S., 2006. Reconstruction of sea surface temperature variations in the Arabian Sea over the last 23 kyr using organic proxies (TEX86 and U37k′). Paleoceanography 21, PA3003. http://dx.doi.org/10.1029/2005PA001215.

Imbrie, J., Hays, J. D., Martinson, D. G., McIntyre, A., Mix, A. C., Morley, J. J., Pisias, N. G., Prell, W. L., Shackleton, N. J., 1984. The orbital theory of Pleistocene climate: support from a revised chronology of the marine $\delta^{18}O$ record. In: Berger, A. L., Imbrie, J., Hays, J.D., Kukla, G., Saltzman, B. (Eds.), Milankovitch and Climate, vol. 1. D. Reidel, Dordrecht, pp. 269e305.

Jorissen, F. J., de Stigter, H. C., and Widmark, J. G. V., 1995. A conceptual model explaining benthic foraminiferal microhabitats, Mar. Micropaleontol., 26, 3–15, doi:10.1016/0377-8398(95)00047-X.

Jung, S. J. A., Kroon, D., Ganssen, G., Peeters, F. and Ganeshram, R., 2009. Enhanced Arabian Sea intermediate water flow during glacial North Atlantic cold phases. Earth Planet. Sci. Lett. 280, 220–228.

Kallel, N., Labeyrie, L., Juillet-Leclerc, A., Duplessy, J. C., 1988. A deep hydrological front between intermediate and deepwater masses in the glacial Indian Ocean. Nature 333, 651–655.

Kessarkar, P. M., Rao, V. P. C., Naqvi, S.W.A., Karapurkar, S.G., 2013. Variation in the Indian summer monsoon intensity during the Bølling-Ållerød and Holocene. Paleoceanography 28, 413e425. http://dx.doi.org/10.1002/palo.20040.

Kiefer, T., McCave, I. N., Elderfield, H., 2006. Antarctic control on tropical Indian Ocean Sea surface temperature and hydrography. Geophysical Research Letters 33, L24612.

Kudrass, H. R., Hofmann, A., Doose, H., Emeis, K., Erlenkeuser, H., 2001. Modulation and amplification of climate changes in Northern Hemisphere by Indian summer monsoon during the past 80 kyr. Geology 29, 63e66.

Lear, C., Rosenthal, Y., Slowey, N., 2002. Benthic foraminiferal Mg/Ca paleothermometry a revised core-top calibration. Geochim. Cosmochim. Acta., 66, 3375–3387.

Lisiecki L. E., Raymo M. E., 2005. A Pliocene–Pleistocene stack of 57 globally distributed benthic $\delta^{18}O$ records. Paleoceanography, 20: PA1003. DOI: 10.1029/2004PA001071.

Liu, X., Z. Liu, S. Clemens, W. Prell, and J. Kutzbach.,2007. A coupled model study ofglacial Asian monsoon variability and Indian Ocean Dipole, J. Meteorol. Soc. Jpn., 85, 1–10.

Lutze, G. F., 1986. Uvigerina species of the eastern North Atlantic. In: van der Zwaan, G.J., Jorissen, F. J., Verhallen, P. J. J. M., von Daniels, C. H. (Eds.), Atlantic-European Oligocene to Recent Uvigerina, Utrecht Micropaleontological Bulletins, vol. 35, pp. 21–46.

Lynch-Stieglitz, J., Fairbanks, R. G., Charles, C. D., 1994. Glacial–interglacial history of Antarctic intermediate water: relative strengths of Antarctic versus Indian Ocean sources. Paleoceanography 9 (1), 7–29.

Madhupratap, M., S. Prasanna Kumar, P. M. A. Bhattathiri, M. Dileep Kumar, S. Raghukumar, K. K. C. Nair, and N. Ramaiah., 1996. Mechanism of the biological response to winter cooling in the northeastern Arabian Sea, Nature, 384, 549–552.

Mahesh, B., Banakar, V. K., Burr, G., 2011. Paired measurements of foraminiferal δ18O and Mg/Ca Ratios of Indian monsoons reconstructed from Holocene to Last Glacial Record. Acta Geologica Sinica 85, 950–956.

Pahnke, K., Goldstein, S. L., Hemming, S. R., 2008. Abrupt changes in Antarctic Intermediate Water circulation over the past 25,000 years. Nature Geoscience 1, 870e874.

Pena, L. D., and S. L. Goldstein., 2014. Thermohaline circulation crisis and impacts during the mid-Pleistocene transition, Science, 345(6194), 318–322.

Piotrowski, A. M., Banakar, V. K., Scrivner, A. E., Elderfield, H., Galy, A., Dennis, A., 2009. Indian Ocean circulation and productivity during the last glacial cycle. Earth Planet. Sci. Lett. 285, 179–189. doi: 10.1016/j.epsl.2009.06.007.

Pourmand, A., Marcantonio, F., Bianchi, T. S., Canuel, E. A., Waterson, E. J., 2007. A 28-ka history of sea surface temperature, primary productivity and planktonic community variability in the western Arabian Sea. Paleoceanogr., 22, PA4208. doi: 10.1029/2007PA001502.

Punyu, V. R., 2015. Palaeoproductivity reconstruction for the Northern Indian Ocean utilizing lipid biomarkers, PhD Thesis, Goa University, Goa, India. Pp. 135.

Rajasree, A., Punyu, V. R., Banakar, V. K., 2019. Last 35,000-year water column temperature and productivity variation in the Eastern Arabian Sea: monsoon and global climate connection. Geo-Mar. Lett. 39, 239–248.

Ramesh, K. V., and R. Krishnan., 2005. Coupling of mixed layer processes and thermocline variations in the Arabian Sea. Journal of Geophysical Research 110:C05005. doi:10.1029/ 2004JC002515.

Ravelo, A. C., & Fairbanks, R. G., 1992. Oxygen isotopic composition of multiple species of planktonic foraminifera: Recorders of the modern photic zone temperature gradient. Paleoceanography, 7(6), 815–831. https://doi.org/10.1029/92PA02092.

Raza, T., Ahmad, S. M., 2013. Surface and deep-water variations in the northeast Indian Ocean during 34–6 ka BP: evidence from carbon and oxygen isotopes of fossil foraminifera. Quat. Int. 298, 37–44. http://dx.doi.org/10.1016/j.quaint.2012.05.005.

Regenberg, M., Steph, S., Nürnberg, D., Tiedemann, R., Garbe-Sch€onberg, D., 2009. Calibrating Mg/Ca ratios of multiple planktonic foraminiferal species with d18O-calcification temperatures: paleothermometry for the upper water column. Earth Planet. Sci. Lett. 278 (3e4), 324e336.

Reichart, G. J., den Dulk, M., Visser, H. J., Van der Weijden, C. H., Zachariasse, W. J., 1997. A 225 kyr record of dust supply, paleoproductivity and the oxygen minimum zone from the Murray ridge (northern Arabian Sea). Palaeogeography, Palaeoclimatology, Palaeoecology 134 (1e4), 149e169.

Reichart, G. J., Lournes, L. J., Zachariasse, W. J., 1998. Temporal variability in the northern Arabian Sea Oxygen Minimum Zone (OMZ) during the last 225,000 years. Paleoceanogr., 13,607–621.

Rickaby, R. E. M., Halloran P., 2005. Cool La Ni˜na during the warmth of the Pliocene? Science, 307, 1948–1952.

Rippert, N., Baumann, K. H., Patzold, J., 2015. Thermocline fluctuations in the western tropical Indian Ocean during the past 35 ka. J. Quat. Sci., 30, 201-210.

Robinson, L. F., and T. van de Flierdt., 2009. Southern Ocean evidence for reduced export of North Atlantic DeepWater during Heinrich event 1, Geology, 37(3), 195–198.

Rohling, E. J., and W. J. Zachariasse., 1996. Red Sea outflow during the Last Glacial Maximum, Quat. Int., 31, 77–83.

Romahn, S., Mackensen., A, Groeneveld., J., Pätzold., J., 2014. Deglacial intermediate water reorganization: new evidence from the Indian Ocean. Climate of the Past 10: 293–303.

Rostek, F., Bard, E., Beaufort, L., Sonzogni, C., Ganssen, G., 1997. Sea surface temperature and productivity records for the past 240 kyr in the Arabian Sea. Deep-Sea Research II 44 (6–7), 1461–1480.

Rostek, F., Ruhland, G., Bassinot, F. C., Muler, P. J., Labeyrie, L., Lancelot, Y., Bard, E., 1993. Reconstructing sea surface temperature and salinity using y18O and alkenone records. Nature 364, 319–321.

Saher, M. H., Peters, F. J. C, Kroon, D., 2007. Sea surface temperatures during the SW and NE monsoon seasons in the western Arabian Sea over the past 20,000 years. Palaeogeogr. Palaeoclimatol. Palaeoecol., 249, 216–228.

Saraswat, R., Nigam, R., Weldeab, S., Mackensen, A., and Naidu, P. D., 2005. A first look at past sea surface temperatures in the equatorial Indian Ocean from Mg/Ca in foraminifera. Geophys. Res. Lett. 32 L24605.

Sarkar, A., S. K. Bhattacharya, and M. M. Sarin., 1993. Geochemical evidence for anoxic deep water in the Arabian Sea during the last glaciation, Geochim. Cosmochim. Acta, 57, 1009– 1016.

Schmiedl, G., Leuschner, D. C., 2005. Oxygenation changes in the deep western Arabian Sea during the last 190,000 years: productivity versus deep water circulation. Paleoceanography 20, PA2008. doi:10.1029/2004PA001044.

Schulz, H., von Rad, U., Erlenkeuser, H., 1998. Correlation between Arabian Sea and Greenland climate oscillations of the past 110,000 years. Nature, 393, 54–57.

Schumacher, S., Jorissen, F. J., Dissard, D., Larkin, K. E., Gooday, A. J., 2007. Live (Rose Bengal stained) and dead benthic foraminifera from the oxygen minimum zone of the Pakistan continental margin (Arabian Sea). Marine Micropaleontology 62, 45e73.

Shackleton, N. J., 2000. The 100,000-year ice-age cycle identified and found to lag temperature, carbon dioxide, and orbital eccentricity, Science, 289, 1897–1902.

Shankar, D., Vinayachandran, P. N., Unnikrishnan, A. S., 2002. The monsoon currents in the north Indian Ocean. Prog. Oceanogr., 52, 63–120.

Shetye, S. R., 1986. A model study of the seasonal cycle of the Arabian Sea surface temperature. J. Mar. Res., 44, 521– 542.

Siddall, M., Rohling E. J., Almogi-Labin A., Hemleben C., Meischner D., Schmelzer I. and Smeed D. A., 2003. Sea-level fluctuations during the last glacial cycle. Nature 423(6942), 853– 858.

Sijinkumar, A.V., Nath, B. N., Clemens, S., 2016. North Atlantic climatic changes reflected in the Late Quaternary foraminiferal abundance record of the Andaman Sea, north- eastern Indian Ocean. Palaeogeogr. Palaeoclimatol. Palaeoecol. 446, 11–18.

Singh, A. D., Jung, S. J., Darling, K., Ganeshram, R., Ivanochko, T., Kroon, D., 2011. Productivity collapses in the Arabian Sea during glacial cold phases. Paleoceanography 26 (3).

Sonzogni, C., Bard, E., Rostek, F., 1998. Tropical sea surface temperatures during the last glacial period: a view based on alkenones in Indian Ocean sediment. Quaternary Science Reviews 17, 1185–1201.

Spero, H. J., Mielke, K. M., Kalve, E. M., Lea, D.W., Pak, D. K., 2003. Multispecies approach to reconstructing eastern equatorial Pacific thermocline hydrography during the past 360 kyr. Paleoceanography 18 (1), 1022. doi:10.1029/2002PA000814.

van Aken, H. M., Ridderinkhof, H., de Ruijter, W. P. M., 2004. North Atlantic deep water in the south-western Indian Ocean, Deep Sea Res., Part I, 51, 755–776.

Von Rad, U., Schaaf, M., Michels, K. H., Schulz, H., Berger, W. H., Sirocko, F., 1999. A 5000-yr record of climate change in varved sediments from the Oxygen Minimum Zone off Pakistan, Northeastern Arabian Sea. Quat. Res. 51, 39–53.

Waelbroeck, C., Labeyrie, L., Michel, E., Duplessy, J. C., McManus, J. F., Lambeck, K., Balbon, E., Labracherie, M., 2002. Sea-level and deep-water temperature changes derived from benthic foraminifera isotopic records. Quat. Sci. Rev. 21, 295–305.

Wang Y. V., Leduc, G, Regenberg, M. N., Andersen, T., Larsen., T. Blanz, R. R. Schneider., 2013. Northern and southern hemisphere controls on seasonal sea surface temperatures in the Indian Ocean during the last deglaciation. Paleoceanography 28: 619–632.

Wang, Y. J., Cheng, H., Edwards, R. L., An, Z. S., Wu, J. Y., Shen, C. C., Dorale, J. A., 2001. A high-resolution absolute-dated late Pleistocene monsoon record from Hulu Cave, China. Science 294, 2345–2348. http://dx.doi.org/10.1126/science.1064618.

Wara, M. W., Ravelo, A. C., and Delaney, M. L., 2005. Permanent El Niño-like conditions during the Pliocene warm period. Science, 309, 758–761.

Woodruff, F., 1985. Changes in Miocene deep-sea benthic foraminiferal distribution in the Pacific Ocean: Relationship to paleoceanography. In: J.P. Kennett (Editor), The Miocene Ocean. Geol. Soc. Am. Mem., 163: 131-175.

You Y. Z., 1998. Intermediate water circulation and ventilation of the Indian Ocean derived from water-mass contributions. J. Mar. Res. 56(5), 1029–1067.

You, Y., 2000. Implications of the deep circulation and ventilation of the Indian Ocean on the renewal mechanism of North Atlantic Deep Water. J. Geophys. Res., 105, 23,895–23,926.

Ziegler, M., Lourens, L. J., Tuenter, E., Hilgen, F. J., Reichart, G. J., Weber, S. L., 2010. Precession phasing offset between Indian summer monsoon and Arabian Sea productivity linked to changes in Atlantic overturning circulation. Paleoceanogr., 25, PA3213, https://doi.org/10.1029/2009PA001884.

http://www.globalweathersystems.com